

RSC Advances



This is an *Accepted Manuscript*, which has been through the Royal Society of Chemistry peer review process and has been accepted for publication.

Accepted Manuscripts are published online shortly after acceptance, before technical editing, formatting and proof reading. Using this free service, authors can make their results available to the community, in citable form, before we publish the edited article. This *Accepted Manuscript* will be replaced by the edited, formatted and paginated article as soon as this is available.

You can find more information about *Accepted Manuscripts* in the [Information for Authors](#).

Please note that technical editing may introduce minor changes to the text and/or graphics, which may alter content. The journal's standard [Terms & Conditions](#) and the [Ethical guidelines](#) still apply. In no event shall the Royal Society of Chemistry be held responsible for any errors or omissions in this *Accepted Manuscript* or any consequences arising from the use of any information it contains.

The analysis of catalytic activity induction and deactivation of PtIn/Mg(Al)O catalyst for propane dehydrogenation reaction

Ke Xia, Wan-Zhong Lang*, Pei-Pei Li, Xi Yan, Ya-Jun Guo*

The Education Ministry Key Laboratory of Resource Chemistry and Shanghai Key Laboratory of Rare Earth Functional Materials, Department of Chemistry and Chemical Engineering, Shanghai Normal University, 100 Guilin Road, Shanghai 200234, China.

* Corresponding author. Tel: +86-21-64321951; Fax: +86-21-64321951.
E-mail address: wzlang@shnu.edu.cn(W.Z. Lang), guoyajun@shnu.edu.cn(Y.J. Guo)

Abstract

The catalytic activity induction and deactivation of PtIn/Mg(Al)O catalyst for propane dehydrogenation reaction are experimentally verified. Numerous physical-chemical characterizations are employed to probe the reasons and structure-activity relationships. The mechanism for the activity induction and deactivation is proposed by a schematic diagram. The XPS results prove that the valence state of In exhibits almost no change during the whole dehydrogenation reaction. In the activity induction period, the average metal particle size of PtIn/Mg(Al)O catalyst presents a decreasing trend, and the specific surface area increases. The crystal phase changes from primary periclase (MgO) to dominant meixnerite ($\text{Mg}_6\text{Al}_2(\text{OH})_{18}\cdot 4\text{H}_2\text{O}$). The coke is mainly deposited on carrier. Nevertheless, in the deactivation period, the metal particles tend to agglomerate and grow up. The specific surface area decreases and crystal phase come back to unique periclase crystal phase. A large amount of coke is formed over the catalyst and part of them covers the active sites. These results lead to the evident decrease of catalytic activity.

Key words: Propane dehydrogenation; Activity induction; Deactivation; PtIn/Mg(Al)O.

1 Introduction

In recent years, conversion of low alkanes to value-added olefins has drawn greater attention, because that the light alkenes are extensively utilized as the raw materials for polymer industry and other commodity chemicals.¹⁻⁴ Currently, studies on propane dehydrogenation (PDH) mainly focus on preparing high-efficiency catalysts to attain a desirable yield of propylene.⁵

It is well-known that the deactivation of the catalysts for alkane dehydrogenation is inevitable owing to the formation of coke and the agglomeration of active metallic particles⁶. However, the increasing catalytic activity rather than deactivation phenomenon was observed in the initial stage of the propane dehydrogenation reaction over $\text{In}_2\text{O}_3/\text{MO}_x$ ($\text{M} = \text{Al}, \text{Zr}$) catalysts by Chen et al.⁷⁻⁹. They verified that such unique phenomenon could be associated with an induction period of developing the active sites attributing to the in situ creation of In^0

species confirmed as the intrinsic active center for dehydrogenation. Similar induction period has also been reported for propane dehydrogenation over $\text{Fe}_2\text{O}_3/\text{Al}_2\text{O}_3$ catalyst¹⁰, which was ascribed to the valence state of Fe species variation. Moreover, it was proposed that MoAl^{11} and $\text{Mo/MgAl}_2\text{O}_4^{12, 13}$ catalysts exhibited similar activity induction for butane dehydrogenation, which was due to the in situ formation of active sites from well-dispersed Mo species under the reaction conditions.

In the last few years, calcined hydrotalcite (referred to as $\text{Mg}(\text{Al})\text{O}$) was proposed as an efficient support for Pt-based catalysts in propane dehydrogenation reaction^{14, 15}. Such materials possess moderate basic properties and high thermal stability. It was reported that $\text{Pt/Mg}(\text{Al})\text{O}$ and $\text{PtSn/Mg}(\text{Al})\text{O}$ catalysts were investigated by Galvita et al.¹⁴ with the aim of understanding the effects of Sn and the formation of coke for ethane dehydrogenation. Akporiaye et al.¹⁶ reported a series of $\text{PtSn/Mg}(\text{Al})\text{O}$ catalysts to optimize the formulation procedure and identify the preparation conditions resulting in the best catalytic performance for propane dehydrogenation reaction. Subsequently, Siddiqi et al.¹⁷ revealed the performance of $\text{Pt/Mg}(\text{Ga})(\text{Al})\text{O}$ catalysts for the dehydrogenation of ethane and propane, and they compared the activity, stability, and coking characteristics of $\text{Pt/Mg}(\text{Al})\text{O}$, $\text{PtGa/Mg}(\text{Al})\text{O}$ and $\text{PtSn/Mg}(\text{Al})\text{O}$ catalysts. Furthermore, Sun et al.¹⁸ and Wu et al.¹⁹ reported novel $\text{Pt/Mg}(\text{In})(\text{Al})\text{O}$ catalysts to examine the effect of reduction temperature on PtIn alloy formation and investigate the effects of In/Pt ratio on the intrinsic performances and coking of $\text{Pt/Mg}(\text{In})(\text{Al})\text{O}$. Of all the reports, it is notable that the investigations were devoted to the optimal catalytic performance through probing the structure-performance relationships, and no activity induction took place over the calcined hydrotalcite (or hydrotalcite-like) supported Pt-based catalysts during the whole dehydrogenation reaction. Nevertheless, an interesting activity induction period was found over the $\text{PtIn/Mg}(\text{Al})\text{O}$ catalyst for propane dehydrogenation in this work.

The objective of this paper is to analyze the variation of the catalytic activity of $\text{PtIn/Mg}(\text{Al})\text{O}$ catalyst for propane dehydrogenation. The $\text{Mg}(\text{Al})\text{O}$ support was first synthesized, and then Pt and In were deposited onto the support to attain $\text{PtIn/Mg}(\text{Al})\text{O}$

catalyst by successive impregnation method. As a reference, PtIn/Al and PtIn/Mg catalysts were prepared similarly. Their catalytic performances are evaluated in propane dehydrogenation reaction. And several analytical techniques including XRD, BET, TEM, XPS and TPO are carried out to explore reasons for variation of catalytic activity.

2 Experimental

2.1 Preparation of catalysts

Calcined hydrotalcite (referred as Mg(Al)O) was prepared by co-precipitation and subsequent heat treatment.¹⁴ Mg(NO₃)₂·6H₂O and Al(NO₃)₃·9H₂O (depending on the desired Mg/Al ratio 4:1) were dissolved in deionized water. Another solution was prepared with certain amounts of Na₂CO₃ and NaOH dissolved in deionized water. Then, the two solutions were slowly added dropwise to a glass flask with stirring at 60 °C for 20 min. The solution pH was kept at approximately 9-10. Afterwards, the mixed solution was aged at room temperature for 18 h. The precipitate was filtered, washed with distilled water to neutrality, and dried in air at 110 °C for 10 h. The dried hydrotalcite (HT) was calcined at 700 °C for 10 h to obtain the calcined support (Mg(Al)O).

The PtIn/Mg(Al)O catalysts were prepared by sequential impregnation method. The calcined support Mg(Al)O was firstly impregnated with InNO₃ aqueous solution, followed by H₂PtCl₆ solution. After each impregnation step, the samples were dried at 50 °C for 3 h and then dried at 120 °C for 2 h, and finally calcined at 550 °C for 4 h. The contents of Pt and In in the catalysts were fixed at 0.6 wt % and 1.5 wt %, respectively. For reference, PtIn/Al and PtIn/Mg catalysts were also prepared similarly, using commercial γ -Al₂O₃ (S_{BET} = 222.0 m²/g) and MgO (S_{BET} = 111.4 m²/g) in powder form as the support, respectively. The spent PtIn/Mg(Al)O catalysts undergoing different reaction time were denoted as PtIn/Mg(Al)O-M (M = 0, 2, 12 and 48 h, M representing reaction time). All raw materials were bought from Sinopharm Chemical Reagent Co., Ltd (China).

2.2 Catalysts characterizations

The X-ray diffraction (XRD) patterns of PtIn/Mg(Al)O-M catalysts were recorded on a Bragg-Brentano diffractometer (Rigaku D /Max-2000) with a monochromatic using Cu $K\alpha$ radiation ($\lambda=1.5418 \text{ \AA}$). The samples were scanned from the 2θ value of 20° to 80° with a scan speed of $4^\circ/\text{min}$. The X-ray tube was operated at 40 kV and 30 mA.

The textural properties of PtIn/Mg(Al)O-M catalysts were measured by N_2 adsorption-desorption at liquid nitrogen temperature with an automatic analyzer (NOVA 4000, Quantachrome, USA). The samples were outgassed for 4h under vacuum at 300°C prior to adsorption. The specific surface areas of the samples were calculated by the Brunauer-Emmett-Teller (BET) method. The Barrett-Joyner-Halenda (BJH) pore size model was used to calculate the average pore diameter upon the adsorption branch of isotherm.

The Transmission Electron Microscopy (TEM) images were captured using a JEM-2010 microscope operated at 200 kV. The reduced samples were prepared by dispersing and sonicating in ethanol, then placing a small drop of this solution onto carbon-film coated copper grids and drying in air before testing. Approximately one hundred individual metal particles were measured to determine the average particle size.

The X-ray photoelectron spectra (XPS) of PtIn/Mg(Al)O-M catalysts were investigated on Perkin-Elmer PHI 5000C ESCA using Al $K\alpha$ radiation. All the samples were prereduced in situ under hydrogen at 580°C for 2.5 h. The binding energies (BE) were calibrated using the C_{1s} level at 284.8eV as an internal standard.

The temperature-programmed oxidation (TPO) experiments were implemented in a programmable temperature system. Prior to TPO analysis, the spent catalysts (0.05g) were purged in flowing N_2 (15 mL/min) at 500°C for 1 h. Then the temperature lowered to 40°C to steady the baseline in this gas flow. Afterwards, the reactor was heated in a mixture of 10% O_2 in He from room temperature (RT) to 800°C at $10^\circ\text{C}/\text{min}$. Finally, a thermal conductivity detector (TCD) cell was used to detect CO_2 .

2.3 Catalytic activity measurements

The propane dehydrogenation reactions were performed in a conventional fix-bed quartz reactor. The catalyst (0.3g) was placed in the quartz reactor and prerduced in H_2 at $580\text{ }^\circ\text{C}$ for 2.5 h before evaluation. The reaction conditions were described as follows: $620\text{ }^\circ\text{C}$ for the reaction temperature, 0.1 MPa pressure, $H_2/C_3H_8/Ar = 7:8:35$ (molar ratio), and the propane weight hourly space velocity (WHSV) is 3.3 h^{-1} . A gas chromatography (GC, SP-6890) equipped with a FID detector and an AT-PLOT PORA-Q capillary column was employed to analyze the outlet gas mixtures. The propane conversion and propylene selectivity were based on the total number of carbon atom balance.

3 Results and discussion

3.1 The activity induction and deactivation phenomena of PtIn/Mg(Al)O catalyst for propane dehydrogenation

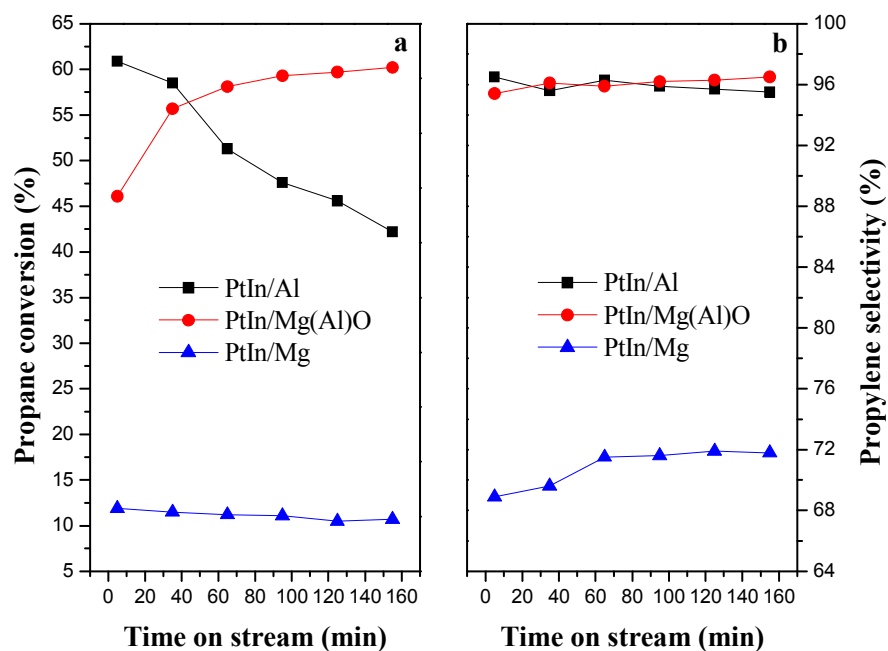


Fig. 1 Propane conversion (a) and propylene selectivity (b) as function of time for different catalysts (reaction conditions: $620\text{ }^\circ\text{C}$, $H_2/C_3H_8/Ar$ (molar ratio) = $7:8:35$, $WHSV = 3.3\text{ h}^{-1}$, $m(\text{cat}) = 0.3\text{g}$).

Fig. 1 exhibits the catalytic performances of the different catalysts. The propane conversions with the time on stream for different catalysts are presented in Fig. 1(a). It can be seen that the PtIn/Al catalyst exhibits the highest initial activity among the three catalysts, but its activity decreases rapidly with increasing time on stream. A low, but stable activity (around 11.0 % propane conversion) can be obtained over PtIn/Mg catalyst. Moreover, as shown in Fig. 1(b), PtIn/Al and PtIn/Mg(Al)O catalysts possess a high selectivity to propylene (about 96.0%). Compared to that, the relatively low selectivity of around 70.0% can be noted over PtIn/Mg sample.

From Fig. 1(a), it is interesting that the catalytic activity of PtIn/Mg(Al)O catalyst increases continually during the whole 155 min reaction, which is inconsistent with the inevitable deactivation of the catalysts for propane dehydrogenation. However, it is noteworthy that this phenomenon cannot be observed over the other two catalysts. On the basis of aforementioned results, it can be concluded that it is peculiar for the Mg(Al)O material supported PtIn bimetallic catalyst to present the constant increasing activity, which should be called as ‘activity induction period’.

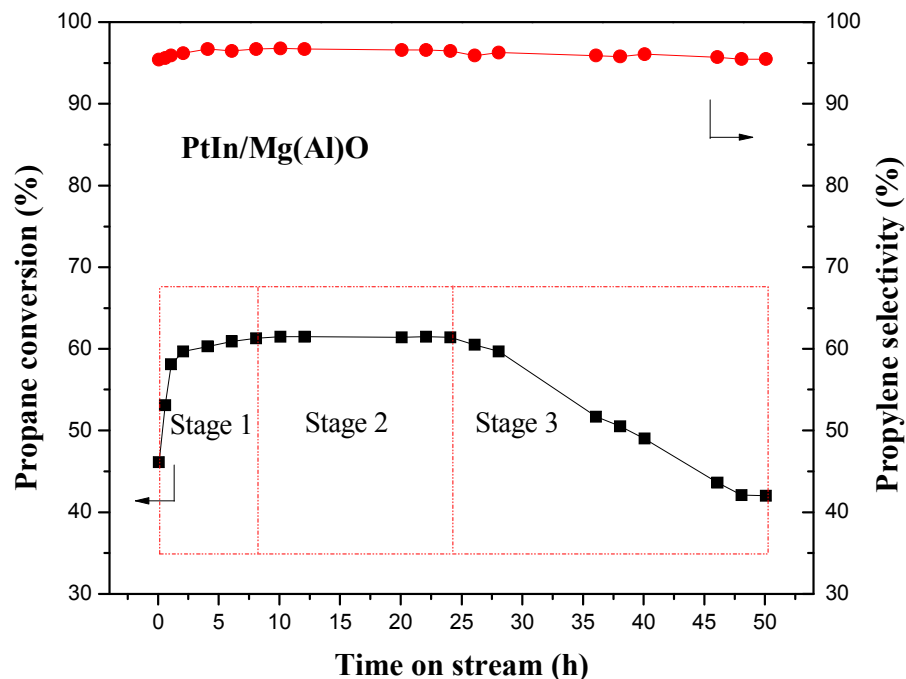


Fig. 2 Stability test of PtIn/Mg(Al)O catalyst in propane dehydrogenation (Reaction conditions: 620 °C, H₂/C₃H₈/Ar (molar ratio) = 7:8:35, WHSV = 3.3 h⁻¹, m(cat) = 0.3g).

To further probe the variation of catalytic activity, the longer reaction time (50 h) of consecutive propane dehydrogenation at 620 °C was investigated over the PtIn/Mg(Al)O catalyst. As can be seen from Fig. 2, the variation of propane conversion can be divided into three stages: ascent stage 1 (0-8 h), stable stage 2 (8-24 h) and descent stage 3 (24-50 h). The initial propane conversion (5min of reaction time) is 46.1%, and it rises constantly until 8 h. Then, it keeps stable at around 61.0% for 16 h. After that, the conversion begins to decline gradually, and final value is 42.0% after 50 h propane dehydrogenation reaction. The propylene selectivity varies little (about 95%) during the whole dehydrogenation reaction process. The spent PtIn/Mg(Al)O catalysts undergoing different reaction time (denoted as PtIn/Mg(Al)O-M, M = 0, 2, 12 and 48 h representing reaction time) were cooled and took out for the following structure analysis and characterizations.

3.2 The analysis of activity induction and deactivation of PtIn/Mg(Al)O catalyst

3.2.1 XPS analysis

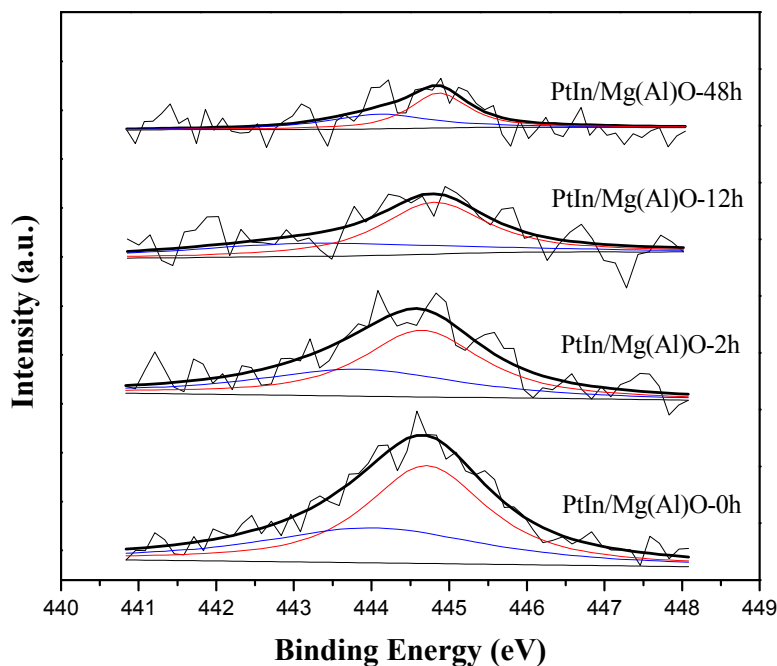


Fig. 3 $\text{In}3d_{5/2}$ XPS spectra of PtIn/Mg(Al)O-M catalysts.

In order to demonstrate surface chemical state of In, the XPS analysis of PtIn/Mg(Al)O catalysts in different stages was carried out. The XPS spectrum of In3d region is showed in Fig. 3 and the semi-quantitative results are summarized in Table 1. It can be seen that the $\text{In}3d_{5/2}$ level is well deconvoluted by two curves at 443.9-444.1 eV and 444.7-445.0 eV, attributing to zerovalent In or PtIn alloy and oxidation state of In^{20} , respectively. As seen in Table 1, the percentages of zerovalent In for the four samples are all approximately 40%, which suggests that the valence state of In on the surface of PtIn/Mg(Al)O catalyst varied little as the reaction proceeds. These results are different from the previous literature⁷, which revealed that the induction period was owing to the creation of surface metallic indium ($\text{In}^{3+} \rightarrow \text{In}$) as the active sites. It is well-known that the coke may influence the detection of the covered In elements especially for low concentration. From Table 1, the In/Pt ratio in PtIn/Mg(Al)O-0h catalyst is 11.6, which is much higher than the value(4.2) calculated from Pt

and In precursors, indicating the enrichment of In_2O_3 on the surface of the catalyst. Fan et al.²¹ also proposed a similar viewpoint. From Fig. 3, it is obvious that the intensity of $\text{In}3d_{5/2}$ XPS peak weakens gradually, this should be due to the surface covering of coke depositions with the extension of the reaction.

Table 1 The semi-quantitative XPS results of PtIn/Mg(Al)O-M catalysts

Samples Name	Binding energy (eV)		In/Pt ^a
	In 3d _{5/2}		
PtIn/Mg(Al)O-0h	444.1(40%)		11.6
	444.7(60%)		
PtIn/Mg(Al)O-2h	443.9(40%)		10.3
	444.7(60%)		
PtIn/Mg(Al)O-12h	443.9(39%)		8
	444.8(61%)		
PtIn/Mg(Al)O-48h	444.1(41%)		4.1
	445.0(59%)		

Note: ^a detected by XPS analysis.

3.2.2 XRD analysis

With the aim of identifying the crystallization phase presented in the samples of different reaction time, X-ray diffraction analysis was implemented. The XRD patterns of PtIn/Mg(Al)O-M samples are depicted in Fig. 4. The fresh catalyst (PtIn/Mg(Al)O-0h) exhibits periclase (MgO) as the primary crystal phase. Additionally, multiple peaks located at $2\theta = 22.5^\circ, 35^\circ, 39^\circ, 46.5^\circ$ and 61.7° are found in the pattern of PtIn/Mg(Al)O-0h sample, which are matched with the characteristic peaks specific to meixnerite $\text{Mg}_6\text{Al}_2(\text{OH})_{18}\cdot 4\text{H}_2\text{O}$ (JCPD No.38-0478).²² The spent catalyst for 2 h reaction time shows a similar pattern as PtIn/Mg(Al)O-0h sample. However, the third curve corresponding to the catalyst of stage 2 (PtIn/Mg(Al)O-12h catalyst) exhibits meixnerite as the dominant crystal phase accompanied

with unobvious peak characteristic of periclase. The phenomenon may be due to that H_2O gas phase formed in the process of propane dehydrogenation with hydrogen leads to the reconstruction of the mixed oxide $(\text{Mg}(\text{Al})\text{O})$.^{23, 24} These results indicate that meixnerite crystal phase of support provides better catalytic performance than that of periclase. Moreover, the unique periclase and little crystals of meixnerite can be obviously observed over the spent catalyst for 48 h reaction, which can be linked with that the catalyst of the descent stage 3 ($\text{PtIn}/\text{Mg}(\text{Al})\text{O}$ -48h) displayed worse activity than others.

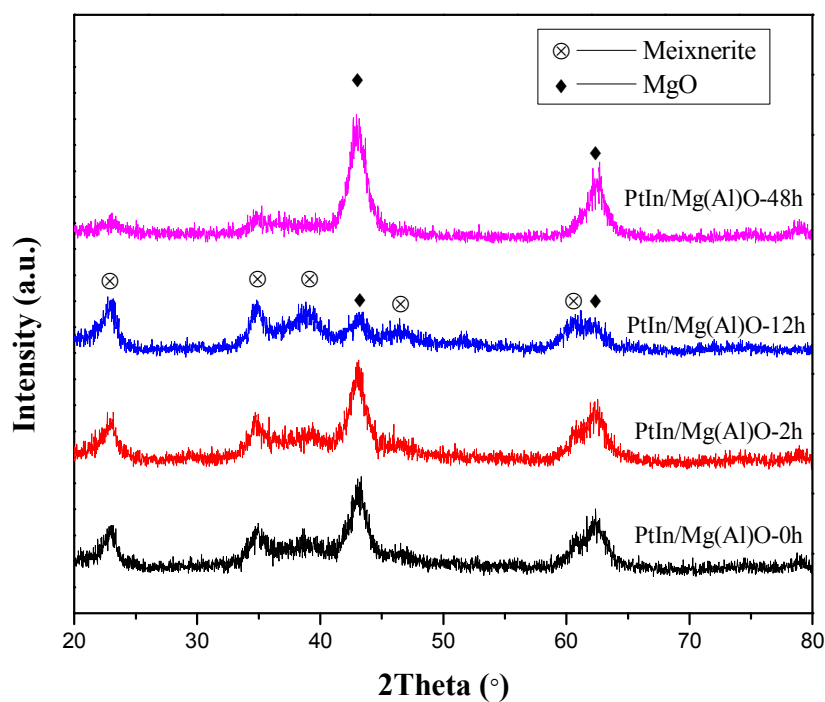


Fig. 4 XRD patterns of $\text{PtIn}/\text{Mg}(\text{Al})\text{O}$ -M catalysts

3.2.3 TEM and BET analysis

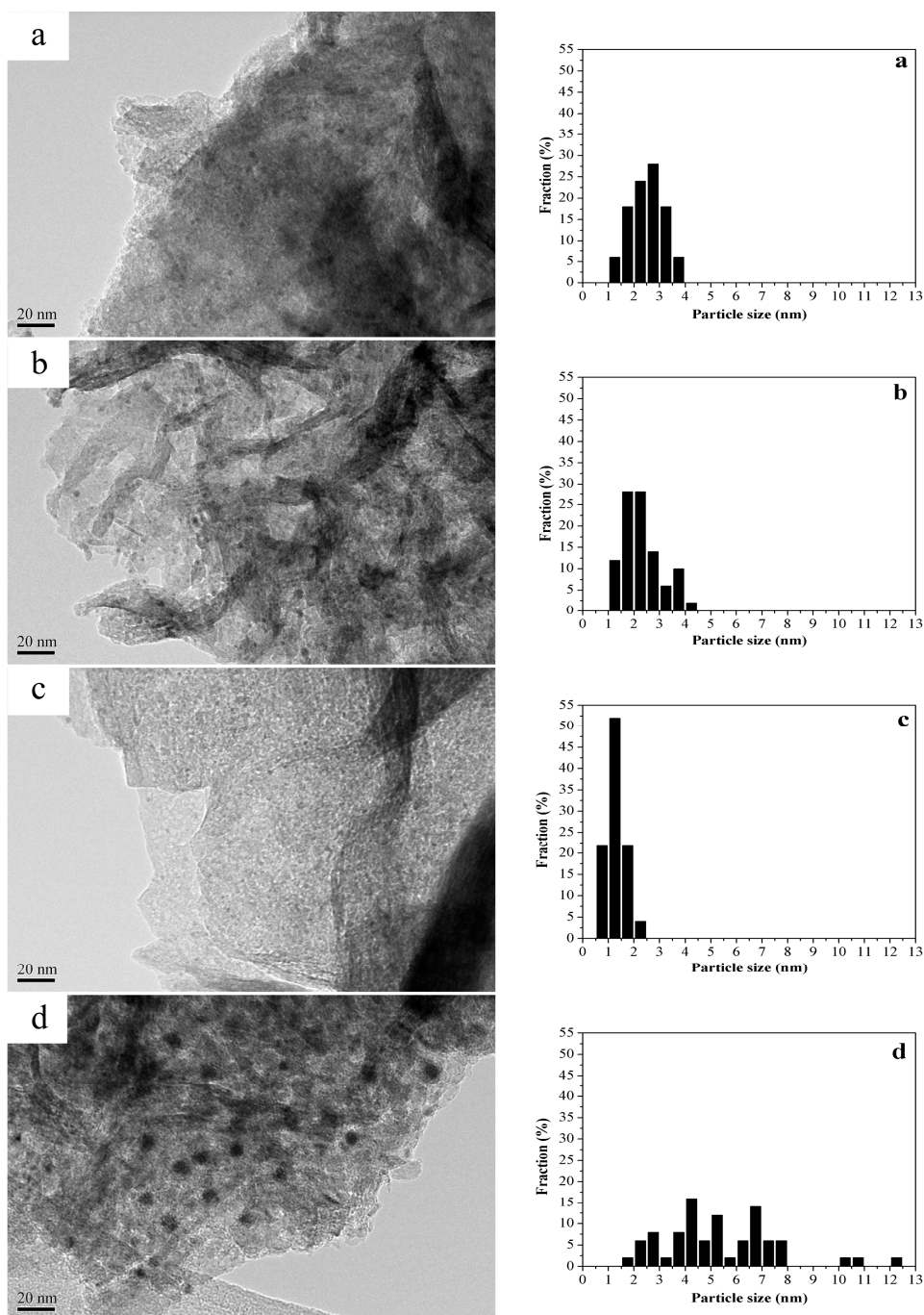


Fig. 5 TEM micrographs of PtIn/Mg(Al)O-M catalysts: (a) PtIn/Mg(Al)O-0h, (b) PtIn/Mg(Al)O-2h, (c) PtIn/Mg(Al)O-12h and (d) PtIn/Mg(Al)O-48h.

TEM micrographs and corresponding metallic particle size distribution of the reduced samples of different reaction time are presented in Fig. 5. The textural properties are summarized in Table 2. It can be observed that the average size of the particles varies

obviously during the reaction process. The PtIn/Mg(Al)O-12h catalyst (corresponding to stage 2 in Fig.2) exhibits a better distribution and the smaller average size of Pt particles (1.3 nm) than other samples. It may be due to Pt particle diffusion of the sample with the highest surface area (279.4 m²/g). Compared to that, the catalyst selected from the descent stage 3 (PtIn/Mg(Al)O-48h) shows the largest particle size of Pt (5.3 nm). It can be explained that the catalyst structure collapse results in the lower surface area and Pt particles tend to agglomerate on the sample surface after running the reaction at high temperature for a long time. All the results indicate that the changes of the surface area and the average Pt particle size of the catalyst are closely related with the variation of catalytic activity.

Table 2 Textural properties of different catalysts

Sample Name	S_{BET} (m ² /g)	V_{p} (cm ³ /g)	D_{p} (nm)	Average Pt particle size (nm)
PtIn/Mg(Al)O-0h	182.9	0.2201	2.818	2.5
PtIn/Mg(Al)O-2h	199.3	0.1798	1.974	2.3
PtIn/Mg(Al)O-12h	279.4	0.2081	1.870	1.3
PtIn/Mg(Al)O-48h	174.4	0.2023	2.157	5.3

3.2.4 TPO analysis

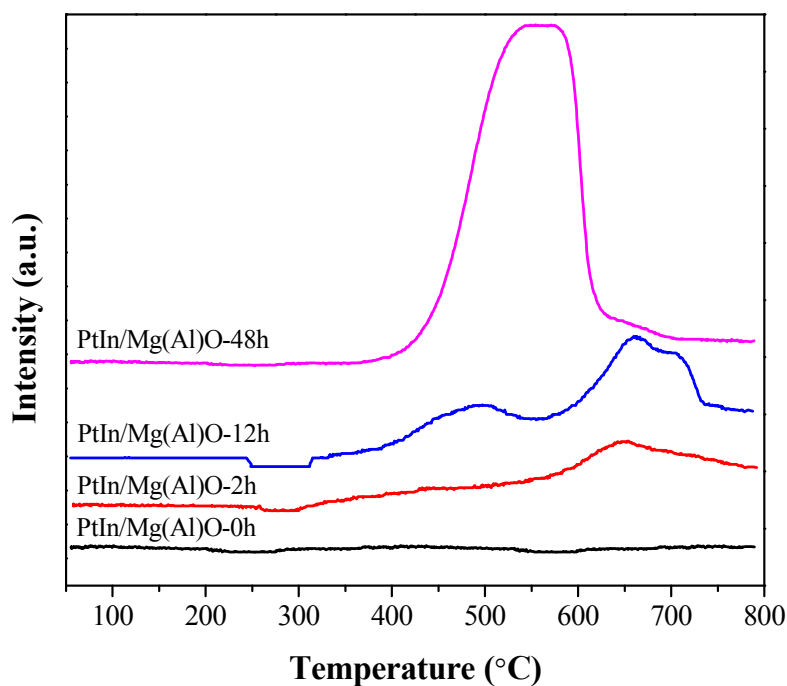


Fig. 6 TPO profiles of PtIn/Mg(Al)O-M catalysts.

The coke deposits produced during the reaction can cover and block the active metal, which is one of the main reasons for the catalyst deactivation.^{25,26} To investigate the nature of coke, temperature-programmed oxidation analysis was implemented. As can be seen from Fig.6, the TPO curves possess two successive peaks, representing coke deposited on the active sites (450-550 °C) and support (600-750 °C), respectively.²⁵ The prerduced fresh PtIn/Mg(Al)O catalyst with no reaction exhibits no peaks of TPO, which is a matter of course. However, the spent sample for 2 h reaction displays a single peak at around 650 °C implying that coke preferentially deposits on the carrier. In contrast, a very small peak located at lower temperature is observed over PtIn/Mg(Al)O-12h catalyst ascribed to the coke deposited on metallic active sites. The phenomena can be easily associated with the fact that no deactivation of the initial eight hours and about 16 h activity stabilization period is shown in Fig. 2. It can be explained that the presence of In can facilitate the coke deposits on the support prior to the active sites, which shows a similar effect as Sn²⁷. Moreover, it should be

noted that for the spent catalyst of 48 h reaction (attaching to the descent stage 3 in Fig. 2), a large amount of coke formed on the active sites due to the increase of the size of the surface Pt ensembles. Zhang et al.²⁸ argued that the hydrocarbon can easily form multiple carbon-metal bonds with large size Pt particles, which leads to more precursors absorbed on the metal surface triggering coke formation.

3.3 The mechanism of activity induction and deactivation of PtIn/Mg(Al)O catalyst

According to the coke deposition and Pt particle size of PtIn/Mg(Al)O catalyst as a function of time on stream, a schematic diagram of mechanism is proposed in Fig. 7. In the above XPS analysis, the enrichment of In_2O_3 on the surface of PtIn/Mg(Al)O catalyst is verified. On the other hand, In promotes the transfer of coke from active sites to support (in TPO analysis), which is similar to the effect of Sn. According to the structure of Pt-SnO_x-support proposed in literature²⁷, Pt metal particles are highly dispersed on the support attributing to a similar “sandwich structure” of Pt-In₂O₃-support. In this case, the average Pt particle size is about 2.5 nm. When the reaction time rises up to 2 h, coke deposition begins to form on the support, and little coke deposited on the metallic active sites, triggering that no deactivation for PtIn/Mg(Al)O catalyst can be found in the initial stage (stage 1). The smallest size of Pt particles over the catalyst can be obtained after 12 h reaction. Here, the main crystalline phase of the carrier changes and results in the higher specific surface area, giving rise to the variation of Pt particles size. Furthermore, with the reaction going on, the average Pt particles agglomerate due to the prolonged high temperature reaction. Thus, the average Pt particle size of 5.3 nm is observed for PtIn/Mg(Al)O-48h. Besides, a large amount of coke is formed over the catalyst and part of them covers the active sites. These results lead to the evident decrease of the catalyst activity.

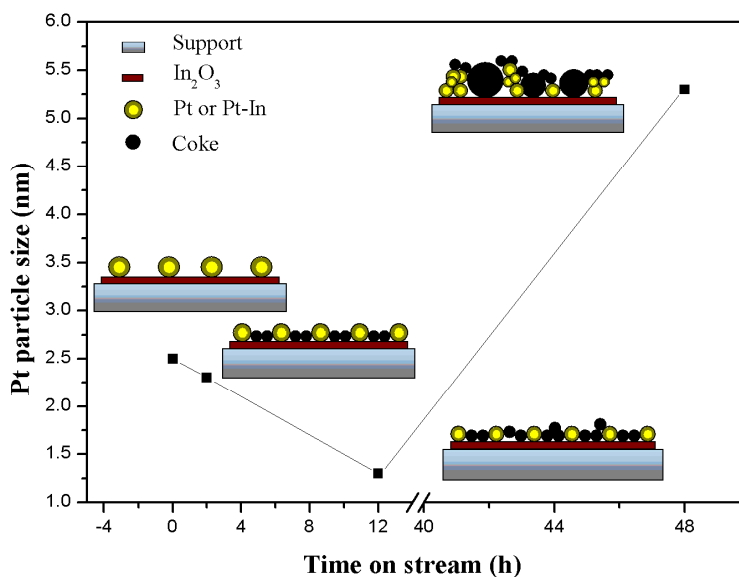


Fig. 7 Schematic of carbon deposition and Pt particle size of prerduced

PtIn/Mg(Al)O catalyst as a function of time on stream.

4 Conclusions

In this work, the Mg(Al)O materials were synthesized by coprecipitation method and used as supports of bimetallic PtIn catalysts for propane dehydrogenation to propylene. A peculiar phenomenon of increasing activity in the initial stage could be observed over the PtIn/Mg(Al)O catalyst. The catalytic activity induction and deactivation of PtIn/Mg(Al)O catalyst for propane dehydrogenation reaction are experimentally verified. XPS results prove that the valence state of In exhibits little change during the whole dehydrogenation reaction. As the reaction proceeded, the smaller metal particle size, the better distribution of Pt particles, the higher specific surface area and the dominant crystalline phase of meixnerite($\text{Mg}_6\text{Al}_2(\text{OH})_{18}\cdot 4\text{H}_2\text{O}$) can be obtained over PtIn/Mg(Al)O catalyst. TPO curves verify that carbon deposits on the support prior to the active sites. However, the agglomeration of metal particles and a large amount of coke formation covering the active sites give rise to marked activity decline after 48 h reaction.

The catalytic activity of PtIn/Mg(Al)O catalyst goes through ascent, stable and descent stages. The activity variation is attributed to the changes of metal particle size, the state of coke deposition, the specific surface area and the crystalline phase of the catalyst.

Acknowledgements

The research is supported by Science and Technology Commission of Shanghai Municipality (13ZR1429900, 14520502900) and International Joint Laboratory on Resource Chemistry (IJLRC).

References

1. R. Grabowski, *Catal. Rev.*, 2006, 48, 199-268.
2. P. P. Sun, G. Siddiqi, M. F. Chi and A. T. Bell, *J. Catal.*, 2010, 274, 192-199.
3. D. Shee and A. Sayari, *Appl Catal a-Gen*, 2010, 389, 155-164.
4. S. Sahebdehfar, P. M. Bijani, M. Saeedizad, F. T. Zangeneh and K. Ganji, *Appl. Catal., A*, 2011, 395, 107-113.
5. Y. B. Xu, J. Y. Lu, M. Zhong and J. D. Wang, *Prog. Chem.*, 2008, 20, 650-656.
6. Z. Nawaz and F. Wei, *J. Ind. Eng. Chem.*, 2010, 16, 774-784.
7. M. Chen, J. Xu, Y. Cao, H.-Y. He, K.-N. Fan and J.-H. Zhuang, *J. Catal.*, 2010, 272, 101-108.
8. M. Chen, J.-L. Wu, Y.-M. Liu, Y. Cao, L. Guo, H.-Y. He and K.-N. Fan, *Appl. Catal., A*, 2011, 407, 20-28.
9. M. Chen, J. Xu, Y. M. Liu, Y. Cao, H. Y. He and J. H. Zhuang, *Appl. Catal., A*, 2010, 377, 35-41.
10. Y. Sun, Y. Wu, L. Tao, H. Shan, G. Wang and C. Li, *J. Mol. Catal. A:Chem.*, 2015, 397, 120-126.
11. M. E. Harlin, L. B. Backman, A. O. I. Krause and O. J. T. Jylhä, *J. Catal.*, 1999, 183, 300-313.
12. G. W. Wang, C. Y. Li, H. H. Shan and W. L. Wu, *Ind. Eng. Chem. Res.*, 2013, 52, 13297-13304.
13. G. Wang, N. Sun, C. Gao, X. Zhu, Y. Sun, C. Li and H. Shan, *Appl. Catal., A*, 2014, 478, 71-80.
14. V. Galvita, G. Siddiqi, P. P. Sun and A. T. Bell, *J. Catal.*, 2010, 271, 209-219.
15. E. A. Redekop, V. V. Galvita, H. Poelman, V. Bliznuk, C. Detavernier and G. B. Marin, *ACS Catal.*, 2014, 4, 1812-1824.
16. D. Akporiaye, S. F. Jensen, U. Olsbye, F. Rohr, E. Rytter, M. Ronnekleiv and A. I. Spjelkavik, *Ind. Eng. Chem. Res.*, 2001, 40, 4741-4748.
17. G. Siddiqi, P. P. Sun, V. Galvita and A. T. Bell, *J. Catal.*, 2010, 274, 200-206.
18. P. P. Sun, G. Siddiqi, W. C. Vining, M. F. Chi and A. T. Bell, *J. Catal.*, 2011, 282, 165-174.

19. J. Wu, Z. M. Peng, P. P. Sun and A. T. Bell, *Appl. Catal., A*, 2014, 470, 208-214.
20. X. Liu, W.-Z. Lang, L.-L. Long, C.-L. Hu, L.-F. Chu and Y.-J. Guo, *Chem. Eng. J.*, 2014, 247, 183-192.
21. X. Q. Fan, J. M. Li, Z. Zhao, Y. C. Wei, J. Liu, A. J. Duan and G. Y. Jiang, *Catal. Sci. Technol.*, 2015, 5, 339-350.
22. P. C. H. Mitchell and S. A. Wass, *Appl. Catal., A*, 2002, 225, 153-165.
23. J. Perez-Ramirez, S. Abello and N. M. van der Pers, *Chem-eur. J.*, 2007, 13, 870-878.
24. M. Mokhtar, A. Inayat, J. Ofili and W. Schwieger, *Appl. Clay. Sci.*, 2010, 50, 176-181.
25. Y. Zhang, Y. Zhou, L. Wan, M. Xue, Y. Duan and X. Liu, *Fuel Process. Technol.*, 2011, 92, 1632-1638.
26. Y. W. Zhang, Y. M. Zhou, J. J. Shi, S. J. Zhou, Z. W. Zhang, S. C. Zhang and M. P. Guo, *Fuel Process. Technol.*, 2013, 111, 94-104.
27. Z. Nawaz, X. P. Tang, Y. Wang and F. Wei, *Ind. Eng. Chem. Res.*, 2010, 49, 1274-1280.
28. Y. W. Zhang, Y. M. Zhou, L. H. Wan, M. W. Xue, Y. Z. Duan and X. Liu, *J. Nat. Gas. Chem.*, 2011, 20, 639-646.